Journal of Computational Neuroscience 11, 111–119, 2001

Efficient and Accurate Time-Stepping Schemes for Integrate-and-Fire Neuronal Networks

MICHAEL J. SHELLEY AND LOUIS TAO*
Courant Institute of Mathematical Sciences, New York University, New York, NY 10012;
Center for Neural Science, New York University, New York, NY 10003
tao@cims.nyu.edu

Received October 11, 2000; Revised May 16, 2001; Accepted June 6, 2001

Action Editor: Carson C. Chow

Abstract. To avoid the numerical errors associated with resetting the potential following a spike in simulations of integrate-and-fire neuronal networks, Hansel et al. and Shelley independently developed a modified time-stepping method. Their particular scheme consists of second-order Runge-Kutta time-stepping, a linear interpolant to find spike times, and a recalibration of postspike potential using the spike times. Here we show analytically that such a scheme is second order, discuss the conditions under which efficient, higher-order algorithms can be constructed to treat resets, and develop a modified fourth-order scheme. To support our analysis, we simulate a system of integrate-and-fire conductance-based point neurons with all-to-all coupling. For six-digit accuracy, our modified Runge-Kutta fourth-order scheme needs a time-step of $\Delta t = 0.5 \times 10^{-3}$ seconds, whereas to achieve comparable accuracy using a recalibrated second-order or a first-order algorithm requires time-steps of 10^{-5} seconds or 10^{-9} seconds, respectively. Furthermore, since the cortico-cortical conductances in standard integrate-and-fire neuronal networks do not depend on the value of the membrane potential, we can attain fourth-order accuracy with computational costs normally associated with second-order schemes.

Keywords: integrate-and-fire networks, accurate time integration schemes, numerical methods

1. Introduction

Simulations of networks of integrate-and-fire point neurons help form the basis for our current theoretical understanding of the properties of large, interacting neuronal systems (see, for instance, Somers et al., 1995; Troyer et al., 1998; McLaughlin et al., 2000, for applications to large-scale visual cortex modeling). While integrate-and-fire dynamics does not account for the detailed generation of action potentials, it does capture an essential feature of neuronal dynamics—namely, individual neurons are coupled to each other through transitory conductance changes associated with spike times. It is therefore important to have numerical schemes that calculate spike times accurately and efficiently.

The discontinuities at firing times are responsible for the highly nonlinear dynamics but may also cause severe numerical errors if not handled correctly. In the integrate-and-fire model, the dynamics of the membrane potentials is an initial value problem after a spike reset. To see where numerical errors arise, consider a scheme with fixed time-steps. Let $t_n = n\Delta t$, and assume that a spike occurs at time $\tilde{t}$ between the t_n and t_{n+1}. Then

$$t_{n+1} - \tilde{t} = A\Delta t, \quad A < 1. \tag{1}$$

*To whom correspondence should be addressed. Address: Courant Institute of Mathematical Sciences, 251 Mercer Street, New York, NY 10012.

After setting the potential at the spike time to the reset potential $v(\tilde{t}) = \hat{v}$, we estimate the value of the true membrane potential at the next time-step as

$$v(t_{n+1}) = v(\tilde{t} + A\Delta t) \approx \hat{v} + Av_t(\tilde{t})\Delta t, \qquad (2)$$

where v_t is the time derivative of v. Therefore, in the naive scheme where we restart the initial value problem at t_{n+1} with initial data $v_{n+1} = \hat{v}$, we immediately introduce an error of order Δt, limiting any time-stepping scheme to first order in time and rendering pointless the use of higher-order time-stepping.

Here we show how to restore accuracy and efficiency to single-step (Runge-Kutta type) integration schemes. Single-step schemes are also amenable to adaptive time-stepping strategies. The main improvement comes from an accurate determination of the spike times and a better estimate of the new initial data v_{n+1}. To deal with these issues, Hansel et al. (1998) and Shelley (used, for instance, in McLaughlin et al., 2000, Pugh et al., 2000) supplemented a second-order Runge-Kutta time-stepping with a simple interpolation scheme to determine the spike times. Using a linear interpolant and the fact that conductances do not depend on the membrane potential, the postspike membrane potentials can be recalibrated to an accuracy of $O(\Delta t^2)$.

Here we analyze and extend this scheme to modify higher-order, single-step integration method. We develop an efficient and highly accurate scheme limited only by the smoothness of the onset of postsynaptic conductance changes. However, it is also this smoothness that allows us to improve efficiency considerably.

We treat synaptic-induced conductance changes of the form

$$G(t - t_{\text{spike}}) = \left(\frac{t - t_{\text{spike}}}{\tau}\right)^m \exp(-(t - t_{\text{spike}})/\tau), \quad t \geq t_{\text{spike}},$$
$$= 0, \quad t < t_{\text{spike}} \qquad (3)$$

where τ is a time constant and m is an integer. In many computational studies of integrate-and-fire neuronal networks, the postsynaptic conductance changes are modeled by an α function (setting $m = 1$; see, for example, Somers et al., 1995) or as the difference between two exponentials with different time constants (e.g., Hansel et al., 1998; Troyer et al., 1998). The latter also has an initial time course that is linear $\approx t - t_{\text{spike}}$ and effectively reproduces the short time behavior of α functions.

It is important to realize that a fundamental limitation on the accuracy of any time-stepping scheme is imposed by the smoothness of the time-derivatives. For integrate-and-fire neurons, this implies a restriction on the form of postsynaptic conductance changes one may use in modeling. Even if one could find spike times as accurately as possible, synaptic-induced conductance time courses of the form of Eq. (3) have only m piecewise continuous time derivatives. Thus the errors after one spike-containing time-step can be no better than $O(\Delta t^{m+1})$, and it is pointless to use a time-stepping scheme with an order of accuracy higher than $m + 1$. Since the biophysically relevant time scale is not set by how smoothly the conductances rise but by how quickly the conductances peak and decay relative to the spike,[1] we choose to model synaptic-induced conductance increases with $m = 5$ to ensure that accurate results can be obtained for rather large time steps.

For postsynaptic potentials of the form in Eq. (3), the additional conductances produced by spikes in the interval (t_n, t_{n+1}) are so small (they are of order $O(\Delta t^{m+1})$) that the intracortical terms do not need to be reevaluated at the start of the new time-step, saving an extra conductance evaluation (if this is of concern). Furthermore, because the conductances in our example system are not voltage dependent, these higher-order schemes cost no more than traditional schemes at half the order. Our modified Runge-Kutta second-order algorithm (RK2) needs one cortico-cortical conductance evaluation per time step and our Runge-Kutta fourth-order scheme (RK4) needs only two evaluations. Since these conductance evaluations are often the most computationally expensive portion of our scheme, the savings are significant.

In the next section we describe our example integrate-and-fire network model and a suitable modification of explicit, single-step integration schemes. The detailed analysis of the numerical integration errors for our algorithm is deferred to the Appendix. In Section 3, we present numerical evidence to support our analysis that the global errors are not dominated by the discontinuous dynamics but by the onset of the synaptic-induced coupling. We end with a discussion of our results.

2. Methods

2.1. The Computational Model

Let v^j be the membrane potential of the jth neuron in a network. Consider a single integrate-and-fire, conductance-based point neuron. Its dynamics can be described by

$$C\frac{dv^j}{dt} = -g_{\text{leak}}(v^j - V_r) - g_e^j(t)(v^j - V_E) - g_i^j(t)(v^j - V_I), \tag{4}$$

where C is the total capacitance, g_{leak} is the leakage conductance, V_r is the rest potential, V_E and V_I are the excitatory and inhibitory synaptic reversal potentials, and $g_e^j(t)$ and $g_i^j(t)$ are the time-dependent conductances arising from input forcing and from the network activity of excitatory and inhibitory neurons. Whenever the potential v^j reaches a threshold $\bar{v}$, that neuron fires, and v^j is reset instantaneously to a reset potential $\hat{v}$. (A refractory period could also be included.)

We take the rest and reset potentials to be equal and use the difference between the threshold and reset to nondimensionalize the potential v. Then using the commonly accepted values (see, for instance, Koch, 1999) of the capacitance ($C = 10^{-6}\,\text{Fcm}^{-2}$), the leakage conductance ($g_{\text{leak}} = 50 \times 10^{-6}\,\Omega^{-1}\text{cm}^{-2}$), the leakage reversal potential ($-70\,\text{mV}$), the excitatory reversal potential ($0\,\text{mV}$), and the inhibitory reversal potential ($-80\,\text{mV}$), we set the values of the reversal potentials and the leakage conductance to be $V_E = \frac{14}{3}$, $V_I = -\frac{2}{3}$, $(g_{\text{leak}}/C) = 50/\text{second}$. Only the time t retains dimension.

We model the time-dependent conductances as arising from external forcing and the network activity of this population of neurons:

$$\begin{aligned} g_e^j(t) &= g_{e0}^j(t) + \sum_k A_{j,k} \sum_l G_e\big(t - t_l^k\big), \\ g_i^j(t) &= g_{i0}^j(t) + \sum_k B_{j,k} \sum_l G_i\big(t - T_l^k\big), \end{aligned} \tag{5}$$

where $t_l^k (T_l^k)$ denotes the time of the lth spike of the kth excitatory (inhibitory) neuron, and $A_{j,k}$ and $B_{j,k}$ are coupling strengths. The input conductances are $g_{e0}^j(t)$ for excitation and $g_{i0}^j(t)$ for inhibition. Both the excitatory and inhibitory postsynaptic conductance functions, G_e and G_i, are given by Eq. (3) but with different time constants.

It is useful to rewrite Eq. (4) as

$$\frac{dv}{dt} = f(t, v) = -\alpha(t)v + \beta(t), \tag{6}$$

where the superscript j has been dropped for clarity. $\alpha(t)$ is the total (nondimensionalized) conductance and is the inverse of an effective integration time scale, and $\beta(t)$ is the (nondimensionalized) "difference current", as it arises as a difference of excitatory and inhibitory currents.

2.2. Modified Time-Stepping Schemes

To improve standard Euler and RK2 methods, Hansel et al. (1998) and Shelley used linear interpolation to approximate the firing times between time-steps. Once the spike times are determined, their values are then used to estimate the potential at $t_n + \Delta t$. For first- and second-order time-stepping schemes, a linear interpolation of spike times is sufficient to preserve the global order of the time-stepping algorithm. In general, as we show in the Appendix, a pth-order time-stepping scheme, coupled with a qth-order spike-time interpolant, has local errors of order $\min(m+1, p+1, q+1)$ and global errors of order $\min(m+1, p, q+1)$, where the dependence on m is imposed by the smoothness of $G(t)$. Thus, the order of the interpolant should be and can be one less than the global order of the time-stepping scheme. Furthermore, for conductance time courses of the form of Eq. (3), neglecting the small conductance changes at the next discretized time, introduces errors of order $O(\Delta t^{m+1})$ and so is consistent with the overall order of the time-stepping. Thus we can improve the efficiency of these schemes by using the previously calculated conductances, saving an extra cortico-cortical conductance evaluation.

To illustrate our approach, consider a modified RK2 scheme. A single RK2 step approximates the changes in the membrane potential by

$$\begin{aligned} v_{n+1} &= v_n + \frac{\Delta t}{2}(k_1 + k_2), \\ k_1 &= f(t_n, v_n) = -\alpha_0 v_n + \beta_0, \\ k_2 &= f(t_n + \Delta t, v_n + k_1 \Delta t) \\ &= -\alpha_1[v_n + \Delta t(-\alpha_0 v_n + \beta_0)] + \beta_1, \end{aligned} \tag{7}$$

where $\alpha_0 = \alpha(t_n)$, $\alpha_1 = \alpha(t_n + \Delta t)$ and similarly for the β's. During an interval not containing any spikes, we

need evaluate $\alpha(t)$ and $\beta(t)$ only once per time-step since $\alpha_0|_{t_n+\Delta t} = \alpha_1|_{t_n}$ and $\beta_0|_{t_n+\Delta t} = \beta_1|_{t_n}$—that is, information can be recycled at the next time-step. Thus the operation count is the same as a first-order algorithm.

Whenever one of new v_{n+1}'s is greater than the threshold $\bar{v}$, that neuron has fired at some time during this last time-step. This spike event contributes (1) to the new initial data v_{n+1} and (2) through synaptic-induced conductance changes, to the membrane potential of every neuron coupled to the spiked one. We address each in turn.

Following Hansel et al. (1998) and Shelley, we use a linear interpolant to estimate the membrane potential between discretized times:

$$v(t) = v_n + \frac{(v_{n+1} - v_n)}{\Delta t} t, \tag{8}$$

setting, without loss of generality, $t_n = 0$. We then approximate the spike time by solving an equation linear in t_{spike}:

$$v(t_{\text{spike}}) = \bar{v} = v_n + \frac{(v_{n+1} - v_n)}{\Delta t} t_{\text{spike}}, \tag{9}$$

whenever v_{n+1} is above the threshold potential for firing.

Having found t_{spike}, we can estimate the value of the postspike membrane potential by asking the following: What are the values of a new $(\tilde{v}_n, \tilde{v}_{n+1})$ pair so that the (interpolated) solution trajectory passes through the *reset potential* $\hat{v}$ at time t_{spike}? The answer corresponds to finding the lower branch in Fig. 1A.

Thus we require the postspike $\tilde{v}_{n+1}$ and a $\tilde{v}_n$ to satisfy two properties: (1) the new membrane potentials are related by a single RK2 step,

$$\tilde{v}_{n+1} = \tilde{v}_n + \frac{\Delta t}{2}(\tilde{k}_1 + \tilde{k}_2), \tag{10}$$

where $\tilde{k}_1 = -\alpha_0 \tilde{v}_n + \beta_0$ and $\tilde{k}_2 = -\alpha_1(\tilde{v}_n + \tilde{k}_1 \Delta t) + \beta_1$; and (2) at time t_{spike} the membrane potential is at reset—that is,

$$\tilde{v}(t_{\text{spike}}) = \hat{v} = \tilde{v}_n + \frac{(\tilde{v}_{n+1} - \tilde{v}_n)}{\Delta t} t_{\text{spike}}. \tag{11}$$

(See Fig. 1A.)

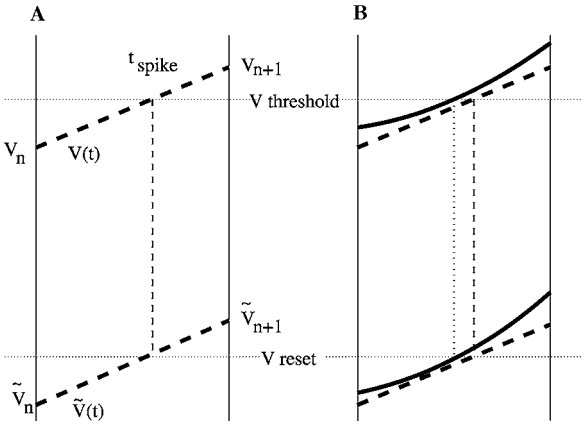

Figure 1. **A:** Recalibration of postsynaptic membrane potential. **B:** Local discretization error analysis. We plot $v(t)$ vs. t: the solid vertical lines are $t = t_n$ and $t = t_n + \Delta t$, and the dotted horizontal lines are $v = \bar{v}$ (top) and $v = \hat{v}$ (bottom). The numerical interpolation is shown as heavy dashed lines. In B, the two "true" solutions are in heavy solid lines. In the text, we denote all values and variables associated with the lower, recalibrated, branch by tildes. For error estimates, see Appendix.

Both of these requirements are linear relations between $\tilde{v}_n$ and $\tilde{v}_{n+1}$. Note that $\tilde{v}_n$ is given explicitly by

$$\tilde{v}_n = \frac{\hat{v} - t_{\text{spike}}(\beta_0 + \beta_1 - \alpha_1\beta_0\Delta t)/2}{1 + t_{\text{spike}}(-\alpha_0 - \alpha_1 + \alpha_0\alpha_1\Delta t)/2}, \tag{12}$$

and $\tilde{v}_{n+1}$ can be found explicitly by substituting Eq. (12) into Eq. (10).

How does this spike influence the dynamics of other neurons in the network? The firing of a neuron increases conductances after the spike time and contributes to $\tilde{k}_2$ in Eq. (10) via corrections to α_1 and β_1. In the Appendix we show that neglecting the postsynaptic conductance increases in α_1 and β_1 leads to errors of order $O(\Delta t^{m+1})$. Therefore, this is consistent with RK2 time-stepping as long as $m \geq 1$, and we can save an extra evaluation of the cortico-cortical conductances.

In general, one step of a single-step method to solve Eq. (6) can be written as

$$v_{n+1} = v_n + \Delta t\, \Phi(t_n, v_n, \Delta t), \tag{13}$$

where the increment function Φ is a linear function of v_n. In our case, to find spike times, we can use an interpolation scheme (e.g., the condition Eq. (11)) that is also a linear relation between v_n and v_{n+1}. Both of these linear relations are the same relations we prescribe for

$\tilde{v}_n$ and $\tilde{v}_{n+1}$, and depend on the fact that the right-hand side of Eq. (6) is linear in the membrane potential v. Since we have determined that the neuron has fired during this time-step, these two linear relations are independent, we can determine the spike time and use it to solve for $\tilde{v}_n$ and $\tilde{v}_{n+1}$ simultaneously.

Thus our algorithm can be extended to higher orders. The standard RK4 scheme is

$$\begin{aligned} v_{n+1} &= v_n + \frac{\Delta t}{6}(k_1 + 2k_2 + 2k_3 + k_4), \\ k_1 &= f(t_n, v_n) = -\alpha_0 v_n + \beta_0 \\ k_2 &= f\left(t_n + \frac{1}{2}\Delta t, v_n + \frac{1}{2}k_1\Delta t\right) \\ &= -\alpha_{1/2}\left(v_n + \frac{1}{2}k_1\Delta t\right) + \beta_{1/2} \\ k_3 &= f\left(t_n + \frac{1}{2}\Delta t, v_n + \frac{1}{2}k_2\Delta t\right) \\ &= -\alpha_{1/2}\left(v_n + \frac{1}{2}k_2\Delta t\right) + \beta_{1/2} \\ k_4 &= f(t_n + \Delta t, v_n + k_3\Delta t) \\ &= -\alpha_1(v_n + k_3\Delta t) + \beta_1, \end{aligned} \tag{14}$$

where $\alpha_0 = \alpha(t_n)$, $\alpha_{1/2} = \alpha(t_n + \Delta t/2)$, $\alpha_1 = \alpha(t_n + \Delta t)$ and similarly for the β's.

To achieve fourth-order time-stepping, it is necessary to add a cubic interpolant for estimating spike times. We use a cubic Hermite polynomial determined by matching the membrane potential and its derivative at the beginning and end of the time-step (v_n; $v_n' = f(t_n, v_n) = -\alpha_0 v_n + \beta_0$; v_{n+1}; and $v_{n+1}' = f(t_n + \Delta t, v_{n+1}) = -\alpha_1 v_{n+1} + \beta_1$). (Note that we have already evaluated the α's and the β's as part of our time-stepping, so we do not need extra conductance evaluations.) Given the membrane potential and its derivative, the interpolation polynomial is

$$\begin{aligned} v(t) = v_n &+ v_n' t \\ &+ \left[\frac{3(v_{n+1} - v_n) - \Delta t(2v_n' - v_{n+1}')}{(\Delta t)^2}\right] t^2 \\ &+ \left[\frac{-2(v_{n+1} - v_n) + \Delta t(v_n' + v_{n+1}')}{(\Delta t)^3}\right] t^3 \end{aligned} \tag{15}$$

(see, for instance, Stoer and Bulirsch, 1983). We then use Newton's method to solve a cubic in t to estimate the spike time $v(t_{\text{spike}}) = \bar{v}$. (This is very efficient and typically we need only two or three iterations.)

To recalibrate the membrane potential after firing, we ask the same question we asked in a RK2 step: What is the new initial value of $\tilde{v}_n$ so that our numerical approximation to the solution passes through the reset potential $\hat{v}$ at time t_{spike}? Since the right-hand side of Eq. (6) is linear in v, (1) a single RK4 step is a linear relation between $\tilde{v}_n$ and $\tilde{v}_{n+1}$, and (2) the Hermite polynomial interpolant is also linear between $\tilde{v}_n$ and $\tilde{v}_{n+1}$. Therefore, as in the RK2 case, we can solve simultaneously for a new $\tilde{v}_n$ and the true postspike membrane potential $\tilde{v}_{n+1}$. Once again we can neglect the immediate postsynaptic potential changes, and this scheme is fourth-order as long as $m \geq 3$.

3. Numerical Results

We solve Eqs. (4) and (5) in a one-dimensional ring of $N = 128$ identical neurons. We drive each neuron with a sinusoid in time, $g_{e0}^j(t) = 25\sin(t)$, and ignore the effects of inhibition ($g_i^j(t) = 0$). The spatial couplings $A_{j,k}$ and $B_{j,k}$ are isotropic Gaussians in the angle separation of neurons along the ring. We then set $\tau_e = 0.6$ milliseconds, and integrate until $t = 1$ second, after each neuron spiked about 11 times. We perform these simulation for a variety of time-stepping schemes to compare their accuracy. We focus on first-order Euler, RK2, RK4 schemes, and their modifications. For Euler and RK2, we use a linear interpolant to find spikes times; for RK4, we use a cubic interpolant.

For error analysis, we determine the membrane potential of a highly accurate, canonical run, where we include the immediate postsynaptic conductance increases, and use our modified RK4 (with a very small time-step $\Delta t = 1.5625 \times 10^{-6}$ seconds). In all cases, the errors are calculated by comparing the membrane potentials to the value of the canonical case at $t = 1$ second: $\text{Error}(\Delta t) = \frac{1}{N}\sum_j |v_{\Delta t}^j(t=1) - v_c^j(t=1)|$ —that is, the average difference between the potentials and the canonical $v_c^j(t)$ at the final time.

First we fix $m = 5$ (as used in Pugh et al., 2000, and McLaughlin et al., 2000) and examine the errors of our modified schemes and the errors associated with standard RK2 and RK4 schemes without recalibration. In Fig. 2, we plot the error as a function of the time-step.

The standard RK2 and RK4 schemes perform no better than our modified Euler scheme, a first-order method. The errors of these schemes are virtually indistinguishable, and each scheme has errors that decrease linearly with step-size (the dotted line is linear in Δt).

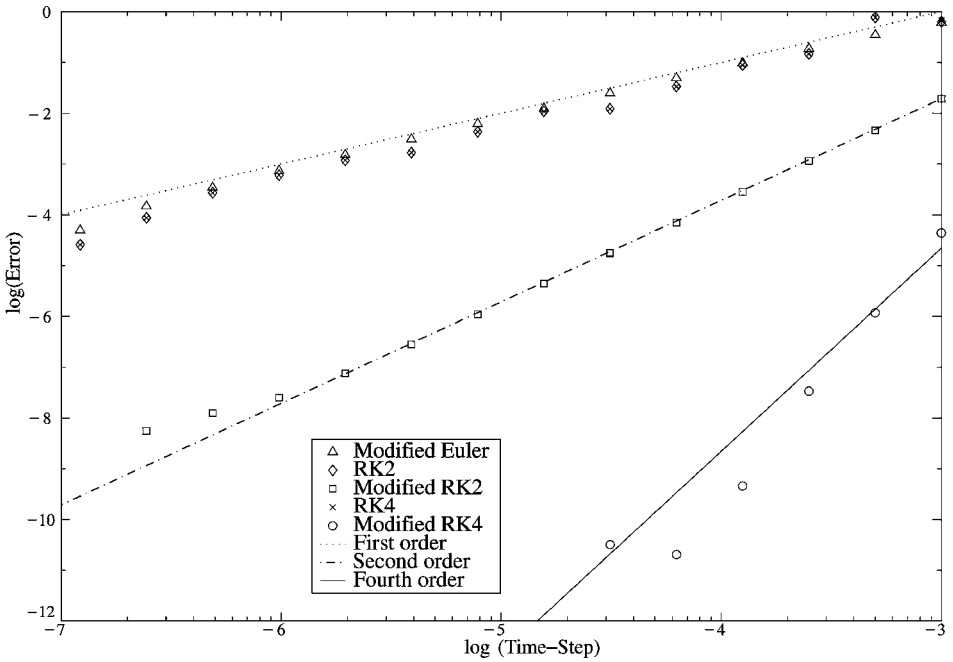

Figure 2. Errors as a function of time-step for different algorithms. Triangles are Euler with linear interpolant, diamonds are RK2, squares are RK2 with linear interpolant, x's are RK4, and circles are RK4 with cubic interpolant. The various lines are not fits but are only guides to the order of convergence. Dotted line is first order, dash-dotted line is second order, and solid line is fourth order.

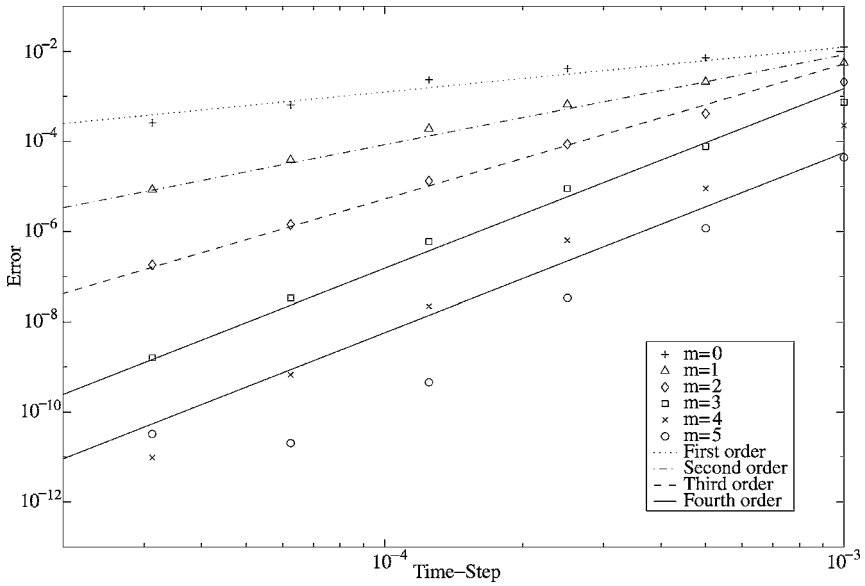

Figure 3. Errors as a function of time-step for different synaptic time courses. The time-stepping is RK4. The data points are crosses: $m = 0$; triangles: $m = 1$; diamonds: $m = 2$; squares: $m = 3$; x's: $m = 4$; and circles: $m = 5$. The lines are not fits. Dotted line: first order; dash-dotted line: second order; dashed line: third order; and solid line: fourth order.

Higher-order accuracy is restored by our modifications. The errors of our modified RK2 scheme decreases quadratically with Δt (as indicated by the dash-dotted line) while the errors of our modified RK4 diminishes as the fourth power of Δt (the solid line). With the fourth-order scheme, we already achieve eight-digit accuracy at a Δt of only 1×10^{-4} seconds. To realize the same accuracy using suitably modified, lower-order schemes requires small time-steps of $\Delta t \approx 10^{-6}$ for RK2 and $\Delta t \approx 10^{-10}$ for first-order schemes.

Next we fix the time-stepping to our modified RK4 scheme and vary the form of the postsynaptic potential changes to demonstrate the limitations of the fourth-order scheme. In Fig. 3, we display the errors for m between 0 and 5. As we discussed previously (and in more detail in the Appendix), the smoothness of the synaptic-induced conductance changes restricts the order of the time-stepping. For $m < 3$, the accuracy of our fourth-order scheme is degraded: The scheme is first order for $m = 0$, second order for $m = 1$, and third order for $m = 2$. Only for $m \geq 3$ do we see fourth-order convergence. These results support the bounds we derived analytically.

4. Discussion

A careful numerical analysis reveals that the global errors of our modified time-stepping methods are regulated by the initial time course of the postsynaptic conductance changes and the spike-time interpolation scheme. Our modifications not only retain properly the convergence order of standard algorithms but are also extremely cost effective. Since it is not necessary to recalculate the cortico-cortical conductances after each firing, the only extra cost comes from the interpolation. In the case of the conductances being voltage independent, higher-order schemes can be constructed with lower-order costs. In taking one RK2 step, one needs only a single evaluation of the functions $\alpha(t)$ and $\beta(t)$ at time $t_n + \Delta t$ ($\alpha_0 = \alpha(t_n)$ and $\beta_0 = \beta(t_n)$ have been evaluated during the previous time-step). Similarly, during one RK4 step, one needs only two evaluations of $\alpha(t)$ and $\beta(t)$ at times $t_n + \Delta t/2$ and $t_n + \Delta t$. Thus, second-order accuracy can be obtained at first-order cost, and fourth-order accuracy at second-order cost.

As shadowing properties of interacting neuronal networks remain an open question, improving accuracy may not be absolutely essential for the numerical simulation of these networks. However, in our current endeavor of building a consistent mathematical picture of the dynamics of interacting neurons, these higher-order schemes facilitate enormously the necessary numerical error estimates. Without higher-order schemes, one can only resort to running first- and second-order schemes at excessively small time-steps (and, hence, for very lengthy CPU times). It is precisely these higher-order error estimates that allow us to conclude whether or not our numerical simulations capture accurately the behavior of the underlying dynamical system.

We note that synaptic-induced conductance increases in the form of an α function, of the difference between two exponentials, or of Eq. (3) can be evaluated indirectly within the framework of a variety of other models (see, for instance, Abbott and van Vreeswijk, 1993; Destexhe et al., 1994; Nykamp and Tranchina, 2000). Our algorithm can accommodate this and also more general forms of postsynaptic conductance changes. Furthermore, although we have restricted the discussion to the case where $G(t - t_{\text{spike}})$ is voltage-independent, our scheme can be extended to the voltage-dependent case. In a recent computational study, Wang (1999) used the second-order scheme of Hansel et al. (1998) to treat NMDA conductances, which can be modeled by voltage-dependent time courses.

We have focused on deterministic models of integrate-and-fire neuronal networks. Similar numerical issues arise when we investigate the effects of noise, say in the form of stochastic conductances and currents, on the dynamics of these networks. Since an accurate determination of spike times is crucial, we need to compute accurate solutions for a given realization of the noise. Unlike studies involving stochastic differential equations, randomness in the conductances and the synaptic currents can be formulated and analyzed in terms of deterministic algorithms and will be the subject of a forthcoming note.

Appendix: Error Estimates

We can modify any pth-order, single-step, time-stepping scheme by using a qth-order interpolant to find spike times and then using the spike times to recalibrate the postspike membrane potentials. Each of our following estimates can be formalized and made rigorous, but we will not do so here. We are content to highlight the main issues involved in these error estimates and to illustrate the various features of our modified time-stepping schemes.

In between neuron firings, the method is pth order so we need only estimate the errors for a spike-containing time-step. During these time intervals, the errors come from three sources: (1) the time-stepping itself, (2) recalibration after neuronal spikes, and (3) neglecting of the conductance increases. Let us address each in turn.

The first, error in the time-stepping itself can be bounded in standard fashion. During a spike-containing time-step, the smoothness of the conductance onset restricts the order of the time-stepping. Consider the effects of synaptic-induced conductance increases on a neuron that has not fired. Postsynaptic conductance changes of the form Eq. (3) have m derivatives, and $m-1$ of them are continuous (the mth derivative being discontinuous at the spike time). Therefore, even if we could determine the spike times as accurately as possible, the error after this time step is bounded by the error in time-stepping and the error we made in the initial conditions:

$$|V(t_n+\Delta t)-v_{n+1}| \le O\left(\Delta t^{\min(m+1,p+1)}\right) + |V(t_n)-v_n|. \qquad (16)$$

The power $m+1$ comes from having m derivatives. Even though the mth derivative is not continuous, it is piece-wise continuous. We can split up this time interval into subintervals using the spike times as the endpoints. Then the mth derivative is continuous on each subinterval, and standard error estimates can be applied to realize this bound.

For a neuron that has spiked during this interval, our scheme determines the spike time and estimates a new v_{n+1}. Let us examine Fig. 1B to facilitate error estimates. Denote the upper branch of the true solution (in heavy solid lines) to Eq. (6) as $V(t)$, with $V_n = V(t_n)$ and the lower branch as $\tilde{V}(t)$, with $\tilde{V}_n = \tilde{V}(t_n)$. Having determined the numerical approximations to the true solution and that this neuron has fired ($v_{n+1} > \bar{v}$), we can use a qth order interpolant (shown in Fig. 1B as a heavy dashed line) to estimate the membrane potential, at any time during this time-step, to within $O(\Delta t^{\min(m+1,p+1,q+1)})$ of the true solution.

How accurately can we determine the spike times? If we can estimate the membrane potential at any time to within $O(\Delta t^{\min(m+1,p+1,q+1)})$, then we should be able to approximate the spike time to the same order. Without loss of generality, assume that the true spike time, $\tilde{t}$, occurs before the estimated spike time, t_{spike} (Eq. (9)). Then we can estimate the spike time to within

$$|\tilde{t}-t_{\text{spike}}| \le \frac{|V(\tilde{t})-v(\tilde{t})|}{\min[f(t,V)]} \le O\left(\Delta t^{\min(m+1,p+1,q+1)}\right), \qquad (17)$$

where the minimum is taken over the true solution during this time interval. Here we have assumed that $f(t,V)$ is bounded away from zero whenever $V=\bar{v}$. Then we can always take the time-step Δt sufficiently small so that $V(t)$ does not go above threshold and then below it in a single time-step.

In estimating the errors along the lower branch, it is important to keep in mind that the linear relations between $\tilde{v}_n$ and $\tilde{v}_{n+1}$ are the same as the ones between v_n and v_{n+1} along the upper branch. So once we have determined $\tilde{v}_{n+1}$, we have determined its value to the same order as we did v_{n+1}:

$$|\tilde{V}(t_n+\Delta t)-\tilde{v}_{n+1}| \le O\left(\Delta t^{\min(m+1,p+1,q+1)}\right) + |V(t_n)-v_n|, \qquad (18)$$

where the dependence on q is an additional limit imposed by how accurately we can determine the spike times.

Finally, we estimate the effects of conductance changes during this time-step. For short times, the synaptic-induced components of $\alpha(t)$ and $\beta(t)$ increase as $(t-t_{\text{spike}})^m$, and we can bound their time integral from the spike time to t_{n+1} by a term of $O(\Delta t^{m+1})$. Thus the error we make by not reevaluating the conductances after a spike is consistent with the overall order of the time-stepping scheme.

Having estimated the local errors incurred during a spike-containing time step, we concatenate these time steps with the time steps during which none of the neurons fired to bound global errors. As we use pth order time-stepping between neuronal firings, the error in the initial conditions just before a spike is bounded by $O(\Delta t^p)$. Therefore, we conclude that our modified scheme (pth order time-stepping, qth order spike-time interpolant) has global errors of

$$|V(T)-v_N| \le O\left(\Delta t^{\min(m+1,p,q+1)}\right) \qquad (19)$$

at $T = N\Delta t$. These error estimates agree exactly with the results of our numerical simulations (presented in Section 3).

Acknowledgments

L.T. acknowledges support by NSF grant DMS-9971813. We thank A. Guillamon, D. Hansel, and D. Nykamp for their critical reading of a preprint of this article.

Note

1. These time-scales can be determined by experimental observations. The typical time scales are of order 3 ms for excitation and 5 ms for inhibition (Azouz et al., 1997; Gibson et al., 1999).

References

Abbott LF, van Vreeswijk C (1993) Asynchronous states in networks of pulse-coupled oscillators. *Phys. Rev. E* 48:1483–1490.

Azouz R, Gray CM, Nowak LG, McCormick DA (1997) Physiological properties of inhibitory interneurons in cat striate cortex. *Cereb. Cortex* 7:534–545.

Destexhe A, Mainen ZF, Sejnowski TJ (1994) Synthesis of models for excitable membranes, synaptic transmission and neuromodulation using a common kinetic formalism. *J. Comp. Neurosci.* 1:195–231.

Gibson JR, Beierlein M, Connors BW (1999) Two networks of electrically coupled inhibitory neurons in neocortex. *Nature* 402:75–79.

Hansel D, Mato G, Meunier C, Neltner L (1998) Numerical simulations of integrate-and-fire neural networks. *Neural Comp.* 10:467–483.

Koch C (1999) *The Biophysics of Computation*. Oxford University Press, New York.

McLaughlin D, Shapley R, Shelley M, Wielaard DJ (2000) A neuronal network model of macaque primary visual cortex (V1): Orientation selectivity and dynamics in the input layer 4Cα. *Proc. Natl. Acad. Sci. U.S.A.* 97:8087–8092.

Nykamp DQ, Tranchina D (2000) A population density approach that facilitates large-scale modeling of neural networks: Extension to slow inhibitory synapses. *Neural Comp.* 13:511–546.

Pugh MC, Ringach DL, Shapley R, Shelley MJ (2000) Computational modeling of orientation tuning dynamics in monkey primary visual cortex. *J. Comp. Neurosci.* 8:143–159.

Somers DC, Nelson SB, Sur M (1995) An emergent model of orientation selectivity in cat visual cortical simple cells. *J. Neurosci.* 15:5448–5465.

Stoer J, Bulirsch R (1983) *Introduction to Numerical Analysis*. Springer-Verlag, New York.

Troyer TW, Krukowski AE, Priebe NJ, Miller KD (1998) Contrast-invariant orientation tuning in cat visual cortex: Thalamocortical input tuning and correlation-based intracortical connectivity. *J. Neurosci.* 18:5908–5927.

Wang X-J (1999) Synaptic basis of cortical persistent activity: The importance of NMDA receptors to working memory. *J. Neurosci.* 19:9587–9603.